Compressive mechanics of warp-knitted spacer fabrics. Part I: a constitutive model

Abstract: This paper presents a theoretical study of the compressive mechanics of warp-knitted spacer fabrics. The first part, as presented in the current paper, focuses on the establishment of a constitutive model which can give accurate stress–strain relationships of warp-knitted spacer fabrics. Based on the analysis of three existing models for polymeric or metallic foams, a constitutive model consisting of seven parameters was firstly proposed for spacer fabrics. The effect of each parameter on the regressive stress–strain curves was then parametrically studied. Experimental validation was finally conducted by using twelve warp-knitted spacer fabrics produced with different spacer monofilament diameters and inclination angles, fabric thicknesses, and outer layer structures to identify the physical sense of the parameters. The analysis has showed that an excellent agreement exists between the regressive and experimental results, and all the seven parameters have quantitatively effect on a particular phase of the resultant stress–strain curves of warp-knitted spacer fabrics. The change of each parameter makes a clear physical sense on the stress–strain curve. Therefore, the proposed constitutive model can be used as a useful tool to engineer the cushioning properties of warp-knitted spacer fabrics. The adoption of the constitutive model to develop a dynamic model for predicting the impact compressive responses of warp-knitted spacer fabrics under various loading conditions will be presented in Part II.

Keywords: warp-knitted spacer fabric, constitutive model, compression, cushioning, stress–strain relationship

1. Introduction

Warp-knitted spacer fabrics comprise two outer layers which are connected together but kept apart by an inner layer of spacer monofilaments.[1] Recently, such kind of fabrics have been

used as cushioning materials in the development of personal protective equipment, laptop sleeves and bags, mattresses, wheelchair cushions, etc.[2] To ensure cushioning materials meeting the desired requirements of specific applications, their stress–strain relationships under specific boundary and loading conditions should be quantitatively engineered and well understood. Some studies have already been made to understand the structure–property relationships of warp-knitted spacer fabrics under quasi-static and impact compressions in planar and spherical forms.[3–9] It has been shown that warp-knitted spacer fabric structures can be engineered to have the key feature of a cushioning material, which can be roughly described by three distinct deformation stages under flatwise quasi-static and impact compressions, i.e. linear elasticity, plateau and densification.[3,4] It has also been reported that a number of factors can affect the compression properties of spacer fabrics, such as spacer yarn inclination angle and diameter, fabric thickness, outer layer structure and yarn material's property.[3] Although some attempts have been made by means of analytical analysis and finite element modeling on the meso-scale, these factors have not been successfully related to the quasi-static compression property quantitatively, due to the highly nonlinear and complex compression deformation of spacer fabric structures.[10–16] In fact, it is even more difficult to theoretically predict the impact responses of warp-knitted spacer fabrics by taking their structural details into account. That is why no dynamic models for predicting the impact behavior of warp-knitted spacer fabric structures can be found in the literature.

Warp-knitted spacer fabrics in current applications are usually subjected to dynamic loading in a curved form such as impact protectors or in a planar form subjected to indentation of various shapes such as wheelchair cushions. To develop such textile products, suitable stress–strain relationships should be tailored to meet the specific requirements of impact protection or shock isolation. This requires several iterations in design, fabrication and quasi-

static/impact testing processes before an optimized design is achieved. To reduce the time and cost in the prototype process, theoretical modelling is always an option. For instance, Du and Hu[6,7] reported an analytical model for predicting the spherical compression properties of warp-knitted spacer fabrics using compression moduli obtained by linearly fitting the flatwise compression stress–strain curves of spacer fabrics in the three stages separately. The linear assumption definitely brings about discrepancies in prediction because the stress–strain curves under flatwise compression are highly nonlinear.

Phenomenological constitutive modeling is a practical and commonly used way to give accurate stress–strain relationships of conventional cushioning materials that are hard to theoretically describe for further analysis and application.[17–19] In this way, empirical formulas linking constitutive model parameters and fabric structural parameters can be established with a large number of experimental data so as to engineer the compression property. A constitutive model giving accurate stress–strain relationships of warp-knitted spacer fabrics for calculations of stress, strain, and absorbed energy is very helpful in conducting the theoretical analysis to develop final products of various shapes under different loading conditions. In particular, since warp-knitted spacer fabrics have been widely used in impact protective applications, it is crucial to understand the impact responses of warp-knitted spacer fabrics under impact with different kinetic energies and contact areas. Hence, the aim of this paper is twofold. Firstly, it is intended to build a constitutive model that can precisely describe the stress–strain relationships of warp-knitted spacer fabrics. Secondly, the purpose is also to establish a dynamic model that can predict the impact responses of warp-knitted spacer fabrics under various impact conditions based on the flatwise compression stress–strain relationships given by the constitutive model. The paper includes two parts. In Part I, a novel constitutive model consisting of seven parameters is firstly introduced. Then, the effect

of each parameter in the constitutive model on the resultant stress–strain curve is parametrically studied. The physical sense of each parameter is also interpreted using experimental validation. In Part II, a dynamic model for predicting the impact compressive responses of warp-knitted spacer fabrics will be developed. It is expected that this study would provide a useful and practical approach to engineer the cushioning properties of warp-knitted spacer fabrics under various loading and boundary conditions.

2. Existing constitutive models

There are many constitutive models in the literature which have been demonstrated to be useful in capturing the mechanical behavior of various structural foams. Liu et al.[17] firstly proposed a nonlinear phenomenological constitutive model consisting of six parameters for structural foams subjected to large deformation, which is described by Eq. (1).

$$\sigma = A \frac{e^{\alpha\varepsilon} - 1}{B + e^{\beta\varepsilon}} + e^{C}(e^{\gamma\varepsilon} - 1) \tag{1}$$

where σ and ε are engineering stress and strain, respectively. The first term in Eq. (1) is for capturing mechanical feature of structural foams in linear and plateau phases, in which A, B, α and β are constants for a given density and strain rate. Parameter A has the unit of stress and the other parameters are dimensionless. The second term including C and γ is used to capture the rapid densification phase of the stress–strain curve of foam in compression. The model has been shown to be successful in fully capturing the three fundamental features of stress–strain response, i.e., linearity, plateau, and densification phases, for structural foams subjected to compression. The constitutive model is also demonstrated to be able to capture the influence of initial density of foams responsible for hardening and softening on the yield plateau phase. Later, Avalle et al.[18] suggested a five-parameter constitutive model, as described by Eq. (2).

$$\sigma = A\left(1 - e^{\frac{-E}{A}\varepsilon(1-\varepsilon)^m}\right) + B\left(\frac{\varepsilon}{1-\varepsilon}\right)^n \tag{2}$$

In addition to capturing the mechanical feature of different structural foams, Parameters E and A also have physical sense, i.e., the elastic modulus and the plateau stress. Most recently, Li et al.[19] reported a constitutive model which is similar to Liu's model but with less parameters for aluminum alloy foams tested at various strain rates, as described by Eq. (3).

$$\sigma = A\frac{e^{\alpha\varepsilon} - 1}{B + e^{\beta\varepsilon}} + C\left(\frac{\varepsilon}{1-\varepsilon}\right) \tag{3}$$

This constitutive model has five parameters, but it has the similar capability to capture the mechanical feature of foams under compression at various strain rates.
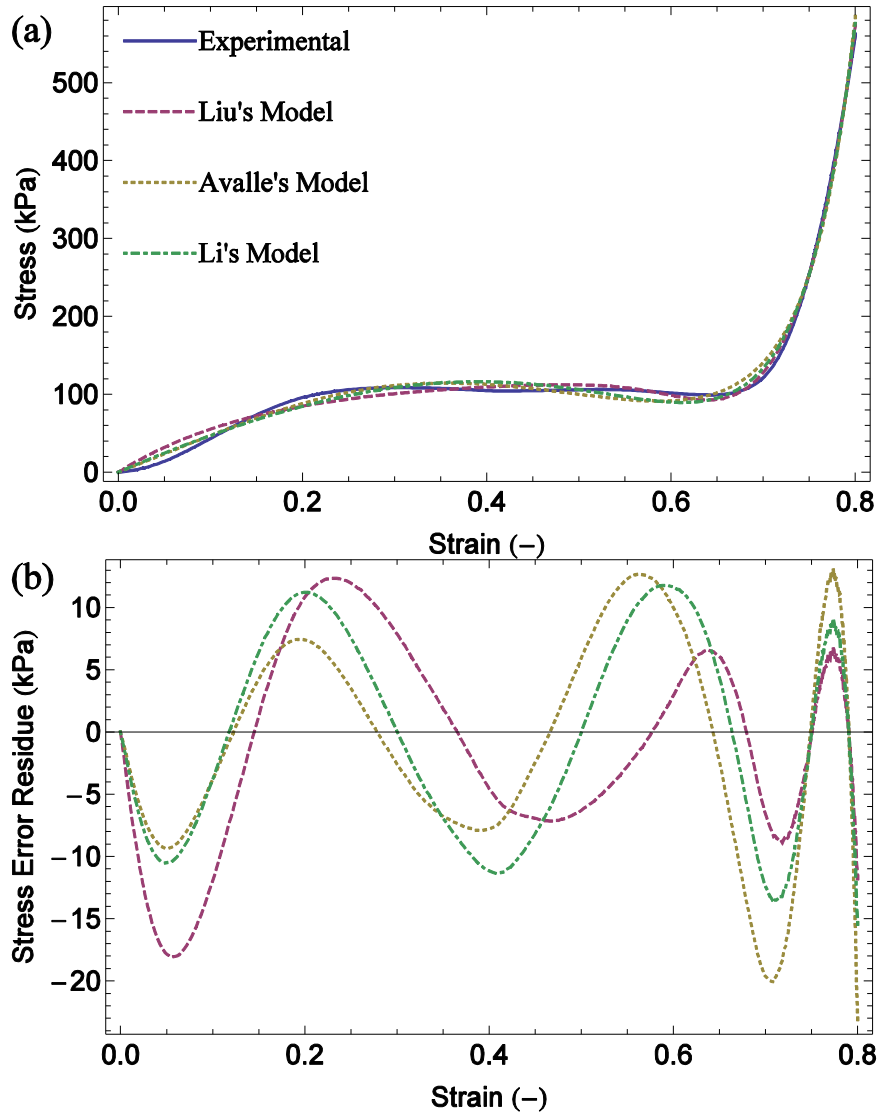
Figure 1. Comparison of stress–strain curves among experimental results and existing constitutive models: (a) stress–strain curves; (b) stress error residue-strain curves.

It has been shown that, similar to structural foams, the overall compression stress–strain relationship of warp-knitted spacer fabrics can be split into three main stages, i.e., linear elasticity, plastic plateau, and densification.[3,5] The deformation mechanisms of the three distinct stages have been identified previously as follows: the linear increase of compression stress in the elasticity stage is due to contact constraints provided by the outer layers to the spacer monofilaments; the long plateau stage is attributed to a combined effect of the shortened effective lengths of spacer monofilaments and their torsion, shear and rotation deformations in postbuckling; the rapid increase of compression stress in the densification stage comes from the collapse and contacts of spacer monofilaments. To examine whether the existing constitutive models are suitable for warp-knitted spacer fabrics, the abovementioned three models were employed to fit the stress–strain curve of a typical warp-knitted spacer fabric under flatwise quasi-static compression. The fitting curves based on these models are shown in Figure 1, where the curve from the experiment is also provided for comparison. It can be found that none of the existing models can well fit the stress–strain curve, since the stress error residues for these models are very large, especially in linear elastic phase and plateau phase. It appears that the experimental curve in elastic phase is concave followed by convex, and the transition between elastic phase and plateau phase is obvious. In addition, the plateau phase of the experimental curve is very flat and long. However, the fitting curves in elastic and plateau phases are all convex, and their transitions are not clear. In this sense, the existing constitutive models are not appropriate to describe the mechanical feature of warp-knitted spacer fabrics. In this regard, to establish a new constitutive model especially suitable for warp-knitted spacer fabric structures is necessary.

3. Proposed model

A newly developed model is here proposed to describe the mechanical feature of warp-knitted spacer fabrics. The formulation is given by Eq. (4).

$$\sigma = A\left(1 - e^{\frac{-E}{A}\varepsilon^{\alpha}\left(1-\varepsilon^{\beta}\right)^{\gamma}}\right) + e^{m}\left(e^{\varepsilon^{n}} - 1\right) \tag{4}$$

where σ and ε are engineering stress and strain, A and E have the unit of stress. Like the existing constitutive models, the first term in Eq. (4) fits the elastic and plateau phases and the second term fits the densification phase. For the first term, it is similar to that of Avalle's model, but two exponential parameters α and β are added to the strain ε. The first term gives a horizontal asymptote for the value of the strain within a certain range of ε as defined by Eq. (5).

$$\lim_{\varepsilon \to \epsilon} A\left(1 - e^{\frac{-E}{A}\varepsilon^{\alpha}\left(1-\varepsilon^{\beta}\right)^{\gamma}}\right) = A \tag{5}$$

where ϵ is supposed to be a value of strain within a certain range. This strain range can be considered as the plateau phase of the stress–strain curve of a warp-knitted spacer fabric structure because over this range of strain the stress is constant and equal to A. ϵ is determined by α, β, γ and n. Hence, A has clear physical sense which is the plateau stress of warp-knitted spacer fabrics. To evaluate the effects of A, E, α, β, γ, m, and n in the proposed constitutive model on the resultant stress–strain curve, a parametric study is conducted as below.

As stated above, Parameter A is defined as the plateau stress in the range of strain ϵ. To investigate the effect of A, three values (100, 200 and 300 kPa) are selected for A and the other parameters are kept constant. The results are plotted in Figure 2. It can be seen that the plateau stresses in the curves exactly equal to the values of A selected. This confirms that the value of A calculated from Eq. (5) is just the plateau stress. It should be noted that the linear

elasticity phase that continuously connects the plateau phase is also affected by A. Unlike the linear elasticity and plateau phases, the densification phase is unaffected by the value change of A. Three values (5, 7 and 9 MPa) are chosen to study the effect of E while the other parameters are kept constant. The results are plotted in Figure 3. It can be seen that E effectively affects the slopes of the curves in the linear elasticity phase, whereas the plateau and densification phases are almost unaffected. From the above analysis, it can be concluded that A successfully define the plateau stress and E controls the modulus of the compression curve.

The effect of α on the stress–strain curves by varying its value from 1 to 2.5 and keeping the other parameters constant is shown in Figure 4. It can be seen that the lower value of α can cause the swifter increase of the stress in the linear elasticity phase. Increasing α also changes the slope of the curve in this phase from convex to concave. Besides, the obvious plateau phases can be observed in the three curves with the same plateau stress regardless of the value of α. It can also be found that the increase of α shrinks the strain range of plateau phase ϵ. However, it appears that α does not affect the densification phases of the stress–strain curves.

Since β and γ are imposed on the same strain symbol, i.e., the second ε of the first term in Eq. (4), their combined effect on the stress–strain behavior is also discussed here. Six combinations of β and γ are selected, and the other parameters are kept constant. The resultant stress–strain curves are plotted in Figure 5. It can be seen that β and γ affect the transition from the plateau phase to the densification phase. Similarly to α, Parameters β and γ also change the strain range of plateau phase ϵ, producing the variation of the stress–strain behavior in this phase from the slope of hardening-like to softening-like. While β is more likely to affect the plateau phase, γ significantly affects the transition between the plateau

phase and densification phase. It should be noted that the linear elasticity phase of the resultant stress–strain curves is unaffected by the value change of β and γ.

The other two parameters m and n are used to capture the rapid densification phase of the stress–strain curve. To investigate their influence on the resultant curve, three values are respectively selected for m and n, while the other parameters are kept constant. The results are plotted in Figure 6 and Figure 7, respectively. It can be found that while m controls the rate of densification, n controls the starting point of the densification phase. The change of m does not affect the elastic and plateau phases, but n significantly affects the strain range of the plateau phase ϵ. Increasing n will extend the plateau phase.

The above parametric study of the seven parameters suggests that the proposed constitutive model is highly effective and adaptive to capture different mechanical features of cushioning materials. While Parameter A has physical sense to represent the plateau stress, each of the other parameters influences a particular phase of the stress–strain curve. This constitutive model can be used to describe the stress–strain characteristics of the whole family of warp-knitted spacer fabrics without composing a dedicated formula for each phase.
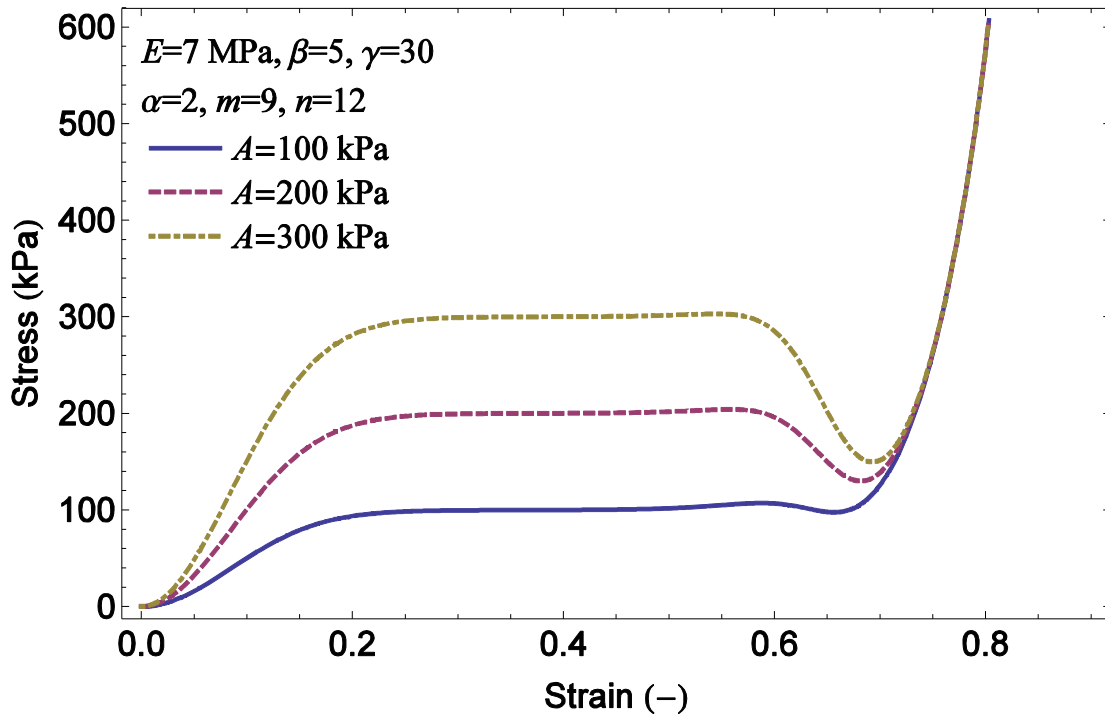
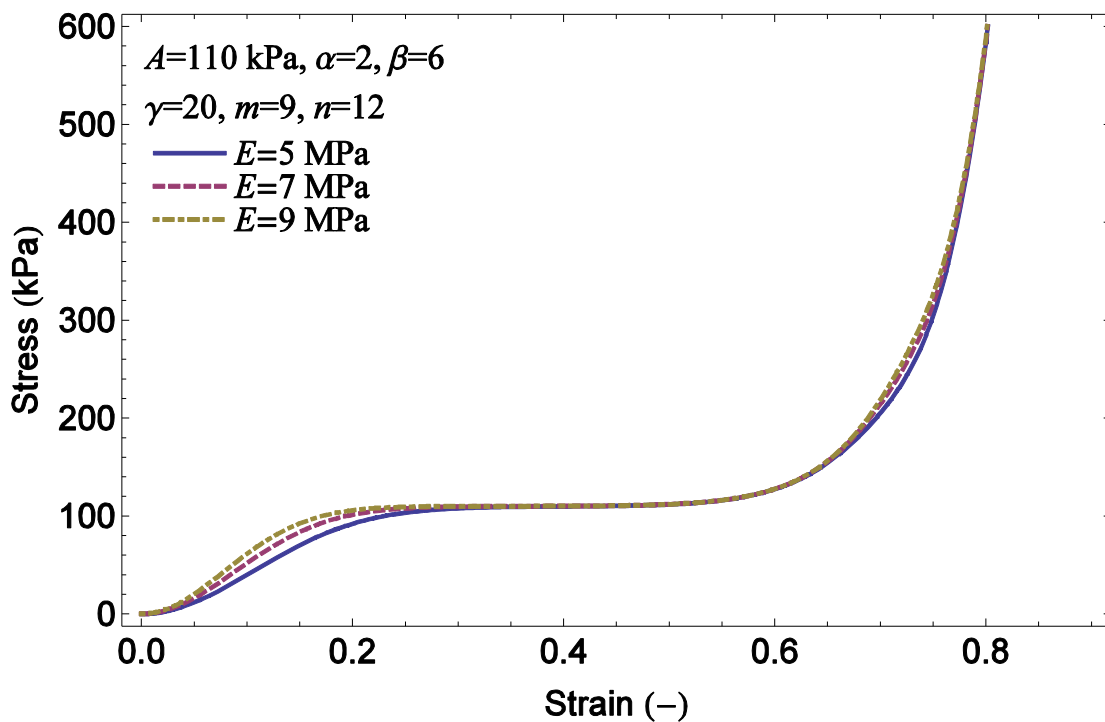**Figure 2.** Effect of Parameter *A* on stress–strain curves.

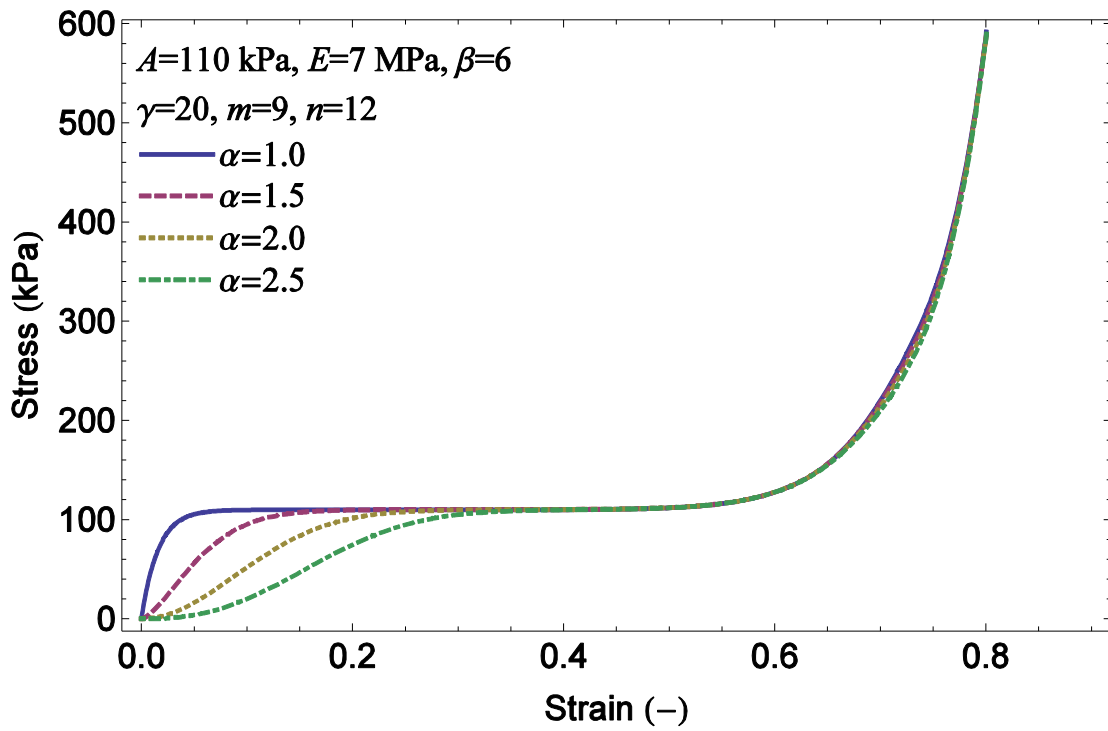**Figure 3.** Effect of Parameter *E* on stress–strain curves.

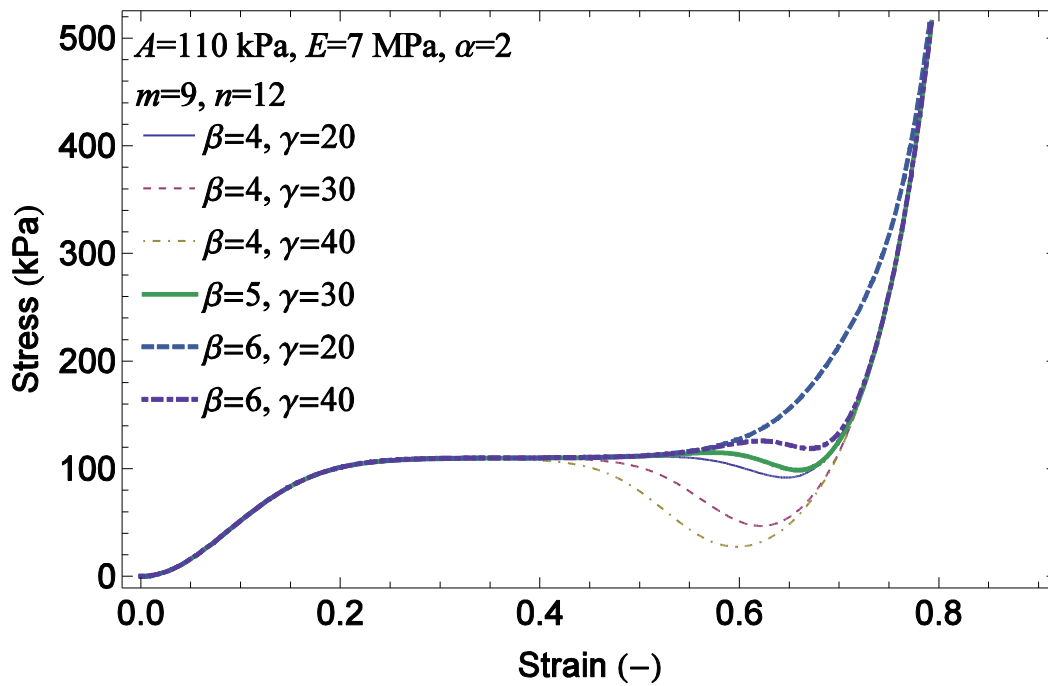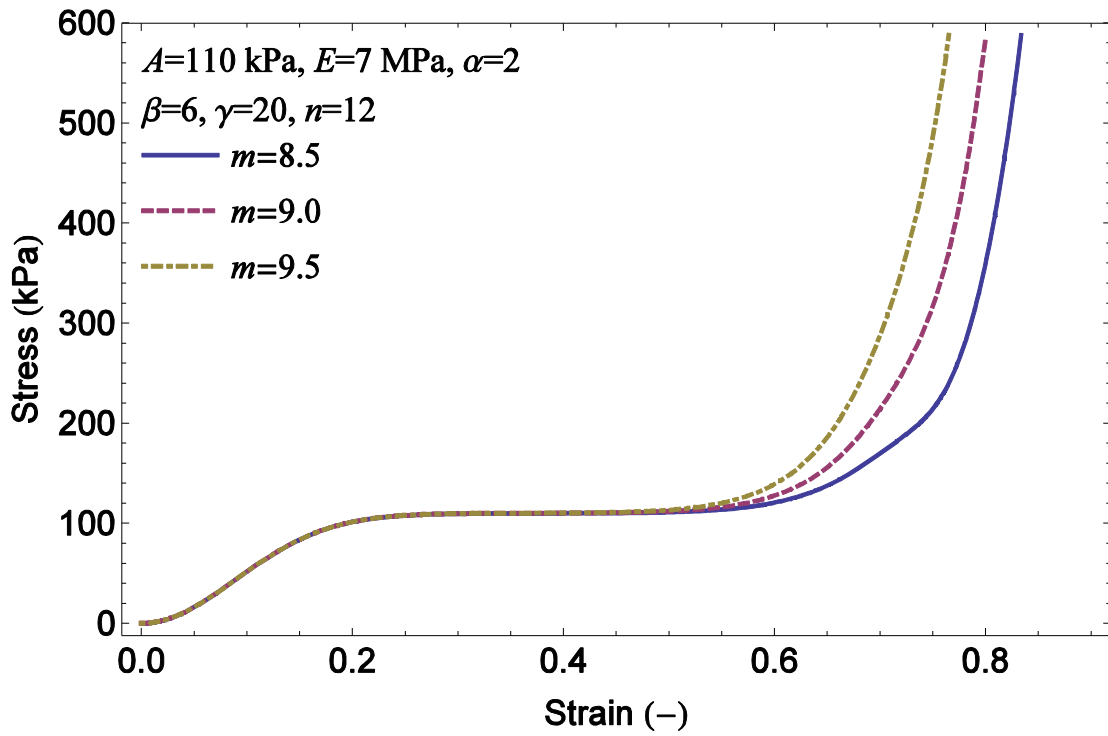**Figure 4.** Effect of Parameter α on stress–strain curves.

Figure 5. The combined effect of Parameters β and γ on stress–strain curves.

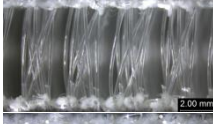**Figure 6.** Effect of Parameter m on stress–strain curves.
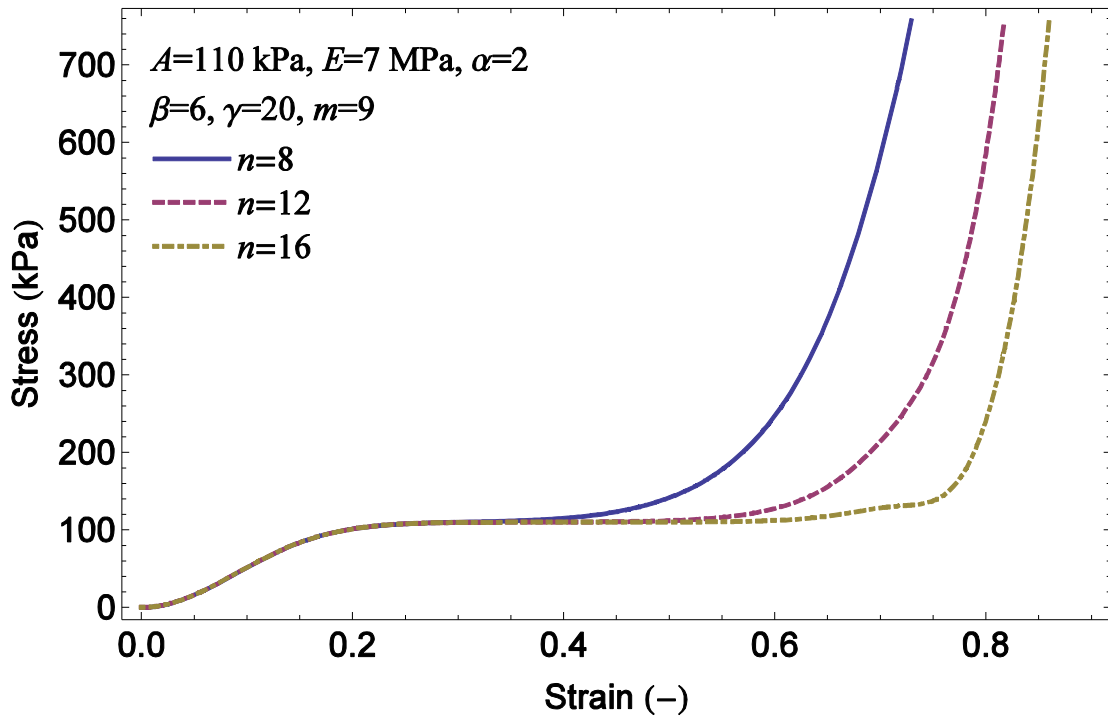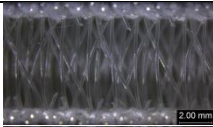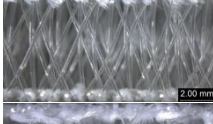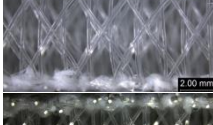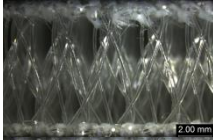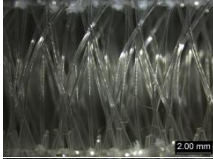
Figure 7. Effect of Parameter n on stress–strain curves.

4. Experimental validation

To verify the capability of the proposed constitutive model, an experimental validation is conducted. Twelve warp-knitted spacer fabrics (S1–S12) produced with different spacer monofilament diameters and inclination angles, fabric thicknesses, and outer layer structures were used for the validation. Table 1 lists the structural details of the fabrics. While the outer layers of all the fabrics were knitted with polyester multifilament of 300 denier (96 filaments), polyester monofilaments of diameter 0.2 mm (400 denier) and 0.16 mm (250 denier) were used for knitting the spacer layers of samples S1–S11 and sample S12, respectively. The compression tests were conducted on an Instron 5566 Universal Testing Machine set up with two 15 cm compression circular plates. The size of all the specimens for testing was 10 cm × 1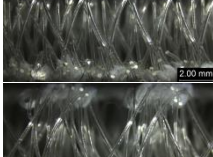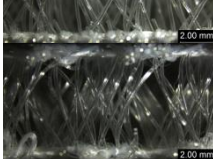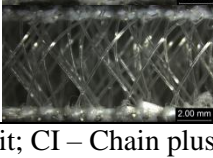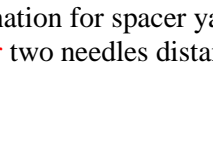0 cm. The tests were carried out at a speed of 12 mm/min up to a deformation of 80% to the initial thickness of the fabrics in an environment of 20 °C and 65% relative humidity. The compression stress–strain curves of these fabrics have already been presented in our previous paper[3] and are adopted here to verify the effectiveness of the constitutive model.

Table 1. Details of spacer fabric samples

Sample No.	Top layer structure	Bottom layer structure	Spacer yarns inclination	Fabric side view	Fabric thickness (mm)	Areal density (g/m^2)	Stitch density (stitches/ cm^2)
S1	L	L	II		7.52 ±0.06	1008.29 ±10.68	41.15
S2	CI	CI	I		7.57 ±0.08	900.11 ±9.01	37.95
S3	CI	CI	II		7.59 ±0.10	901.75 ±14.58	37.26
S4	CI	CI	III		7.40 ±0.06	923.20 ±8.44	37.95
S5	CI	CI	II		5.64 ±0.03	790.63 ±14.51	34.98

S6	CI	CI	II		8.45 ±0.09	1022.08 ±13.38	43.50
S7	CI	CI	II		10.62 ±0.10	1010.42 ±8.83	37.95
S8	RM	CI	II		7.20 ±0.05	830.05 ±11.53	39.33
S9	RM	RM	II		7.76 ±0.06	907.24 ±17.07	51.10
S10	HM	CI	II		7.56 ±0.08	812.70 ±6.61	37.95
S11	HM	HM	II		7.62 ±0.06	724.82 ±8.34	38.86
S12	CI	CI	III		7.06 ±0.09	746.53 ±6.81	39.44

Designation for outer layer structure: L – Locknit; CI – Chain plus Inlay; RM – small-size Rhombic mesh; HM – large-size Hexagonal mesh. Designation for spacer yarn inclination: I – underlapping over one needle distance; II – underlapping over two needles distance; III – underlapping over three needles distance.

Since the proposed constitutive model defined by Eq. (4) is highly nonlinear, the determination of the seven parameters is a rather difficult task. Thanks to the advance of computational power, the nonlinear fitting function *FindFit* built in Mathematica® could be used to successfully fit the model with experimental data at a high accuracy. Function *FindFit* works by searching for values of parameters that yield the best fit. It produces the least-residual sum of squares (RSS) fits (Eq. (6)), which is used to minimize the calculating error.

$$\mathrm{RSS} = \sum_{i=1}^{n}(y_i - \hat{y}_i)^2 \tag{6}$$

where y_i is the ith value of the variable to be predicted and $\hat{y}_i$ is the predicted value of y_i. Since the number of data point is not identical for each fabric, an additional statistical quantity called root mean square error (RMSE) (Eq. (7)) is also calculated for better comparison among fabrics.

$$\text{RMSE} = \sqrt{\frac{\sum_{i=1}^{n}(y_i - \hat{y}_i)^2}{n}} \qquad (7)$$

To illustrate the capability of this new proposed constitutive model, six representative experimental curves covering all characteristics of stress–strain behaviors of the studied spacer fabrics together with their fitting curves are plotted in Figure 8. It can be seen that an excellent agreement between the regressive curves and experimental results is obtained, and the stress error residues of the predicted results are small, especially in linear elastic phase and plateau phase. The statistical results of the fits for all the spacer fabrics are listed in Table 2 together with those from the abovementioned three existing constitutive models for comparison purpose. A direct comparison of the global fitting capability of the models can be performed by means of the RSS and RMSE for each kind of spacer fabric. The comparison shows that the newly proposed model has the best fitting for all the fabrics because of the lowest values of RSS and RMSE.

Table 2. Comparison of the statistical results among the existing and proposed constitutive models

Sample	Liu's model		Avalle's model		Li's model		Proposed model	
	RMSE	RSS	RMSE	RSS	RMSE	RSS	RMSE	RSS
S1	7.3513	23292.16	9.1105	35773.72	7.8786	26753.43	2.8845	3586.02
S2	7.1668	23729.59	11.1956	57908.23	6.9222	22137.28	3.9273	7125.61

S3	5.8254	14218.74	6.7139	18887.20	6.5730	18102.76	1.5391	992.57
S4	6.426	17054.35	7.7598	24868.73	7.3178	22116.25	1.4812	906.12
S5	12.5842	65720.30	14.482	87037.90	11.303	53015.26	6.1482	15687.02
S6	6.7813	21291.84	8.1449	30715.57	6.7431	21052.27	2.2145	2270.54
S7	2.6083	3095.46	1.6468	1234.00	2.9772	4032.95	0.6277	179.30
S8	4.4139	7325.63	5.7382	12380.72	7.1408	19172.47	2.0013	1505.90
S9	2.2439	1883.18	4.1926	6574.12	6.9104	17859.62	1.4270	761.58
S10	2.7544	2738.87	3.8841	5446.21	7.0158	17768.79	0.6995	176.65
S11	3.1275	3677.70	2.2644	1927.92	3.3232	4152.49	1.5478	900.73
S12	2.0508	1505.71	4.1653	6211.11	3.9177	5494.63	0.7451	198.73
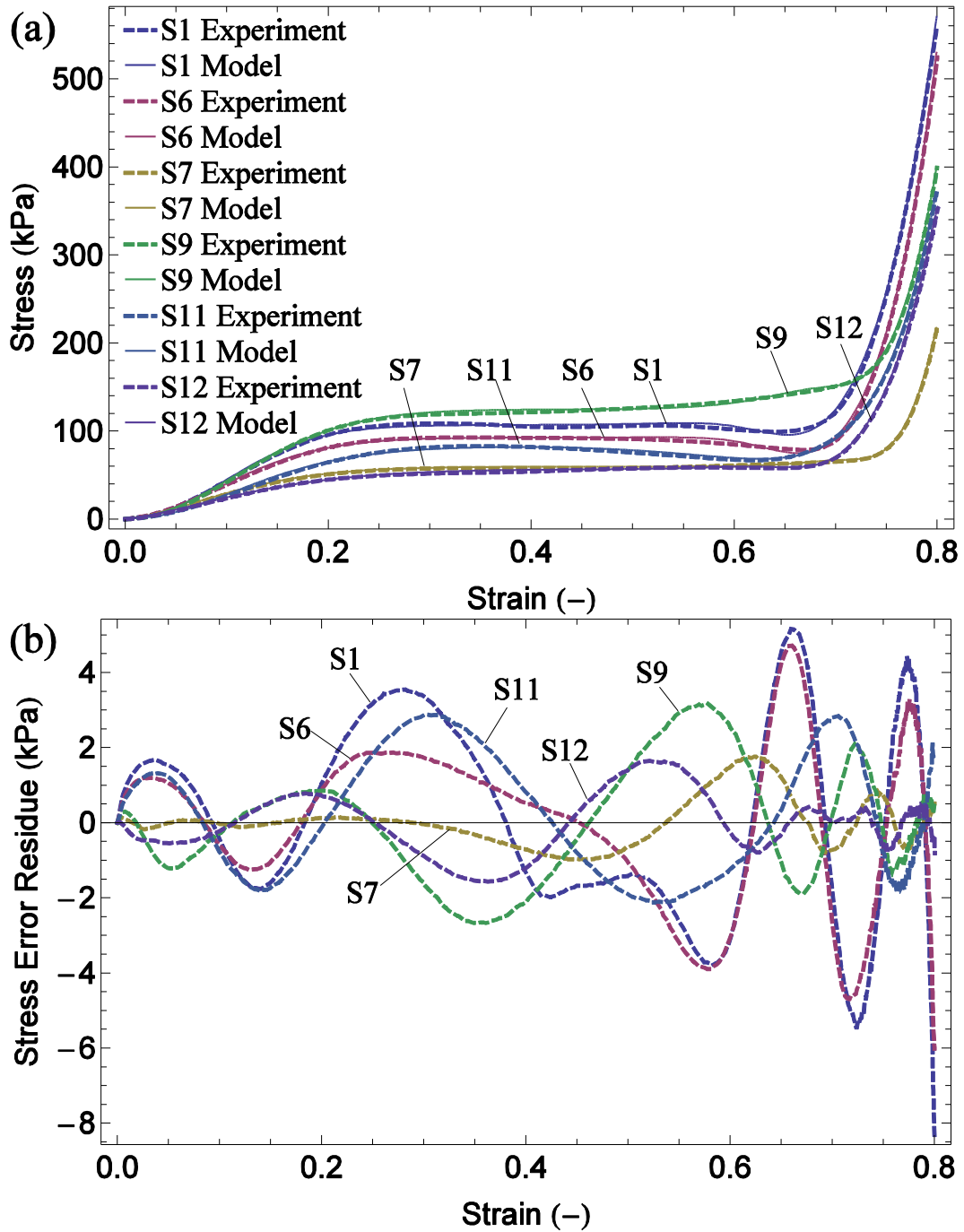
Figure 8. Comparison of stress–strain curves between the experiment and the proposed constitutive model: (a) stress–strain curves; (b) stress error residue–strain curves.

An in-depth understanding of the effect of the seven parameters in Eq. (4) on the fitting stress–strain curves is important to master the constitutive model as a useful tool for engineering the cushioning properties of warp-knitted spacer fabrics. The parameters that

were determined from the fitting process for the spacer fabrics are listed in Table 3. The fitting results show that A for each of the twelve spacer fabrics is close to the real plateau stress. This finding proves that A has the physical sense of the plateau stress. Meanwhile, E is particularly sensitive to the fabric thickness and spacer yarn diameter. For instance, the thinnest spacer fabric S5 with the greatest E has the highest initial modulus due to its shortest spacer monofilaments. On the contrary, the spacer fabric S12 having the lowest E was knitted with the finer spacer monofilament (0.16 mm in diameter) compared with the other fabrics (0.2 mm in diameter) and therefore has the lowest initial modulus.

Figure 8 shows that the slopes of the stress–strain curves of the spacer fabrics in the linear elasticity phase can be changed from foam-like convex (S7 and S12) to concave (S1, S6, S9, S11). Table 3 also indicates that, except for S7 and S12 with α close to 1.5, the values of α for the other spacer fabrics are around 2. This is because S7 with the highest thickness and S12 with the thinnest spacer monofilament are softer than the other spacer fabrics. The slopes of the stress–strain curves of the two fabrics in the linear elasticity phase are convex and softening-like. This proves that α is effective in controlling the slopes of the stress–strain curves in the linear elasticity phase. By manipulating the value of α, various types of linear elasticity phase can be achieved. It should be noted that S7 and S12 has lower E than other spacer fabrics. Thus, E and α are two indices to assess the stiffness of warp-knitted spacer fabrics.

The stress–strain behavior of a warp-knitted spacer fabric in the plateau phase depends on its spacer monofilament inclination angle. Big spacer monofilament inclination angle with the outer layers makes the spacer fabric less stable and shear can easily take place between the two outer layers. This results in a softening-like plateau phase. On the other hand, the plateau

phase of a warp-knitted spacer fabric can also be hardening-like, when its spacer monofilaments have small spacer monofilament inclination angles with the outer layers. Parameters β and γ are two measures to evaluate the slope of the stress–strain curve in the plateau phase. From the fitting results, it appears that when β is less than 5, the corresponding spacer fabric behaves softening-like slope in the plateau phase. In contrast, if β is greater than 5, the relevant spacer fabric possesses hardening-like slope in the plateau phase. Nonetheless, γ is not directly connected with the slope of the stress–strain curve in the plateau phase, but it significantly affects the transition between the plateau phase and densification phase. By examining the experimental curves, it appears that when γ is small, the transition is smooth without inflection. Conversely, if there is a stress drop in the transition phase due to shear of spacer monofilaments, γ is large. This suggests that by manipulating the values of β and γ, various types of plateau phase can be easily achieved to obtain a good fit for the spacer fabrics with different mechanical features. It is highly adaptive to fit the stress–strain behavior of warp-knitted spacer fabrics with a wide range of structures.

The discussion about the effect of m on the resultant stress–strain curve in the parametric study has indicated that it controls the rate of densification. The results in Table 3 show that m for all the spacer fabrics are close to 9. The spacer fabric S7 has the highest value of m due to its highest thickness, leading to the lowest rate of densification. On the contrary, the thinnest spacer fabric S5 has the highest rate of densification and therefore its m is the lowest one among all the spacer fabrics. Thus, the fitting results verify the assertion that m is a direct measure to assess the rate of densification of warp-knitted spacer fabrics.

Finally, Parameter n is to control the starting point of the densification phase. In other words, the value of n determines the strain range of the plateau phase. The fitting results clearly

show that a greater *n* produces a long plateau phase. Conversely, a short plateau phase is related to a low value of *n*. For instance, the thickest spacer fabric S7 has the highest value, while the thinnest spacer fabric S5 has the lowest value of *n*. Hence, it is undoubted that Parameter *n* does control the starting point of the densification phase and plays a key role in fitting the stress–strain relationships of warp-knitted spacer fabrics with different thicknesses because fabric thickness mainly determines the strain range of the plateau phase. For instance, the fabrics S5, S3, S6 and S7 with the same fabric structure but with different thicknesses (5.64, 7.59, 8.45 and 10.62 mm) have the values of 8.9678, 13.4288, 14.3211 and 19.8202, respectively. Therefore, a clear linear relationship between the fabric thickness and *n* is found.

Table 3. Parameters obtained for the warp-knitted spacer fabrics studied

Sample	Parameters						
	A (kPa)	*E* (kPa)	*α*	*β*	*γ*	*m*	*n*
S1	106.3788	6876.8360	2.0869	4.3989	22.5313	9.0573	12.2939
S2	110.1289	5449.1342	1.9105	3.2795	16.3236	8.9417	11.1645
S3	101.3675	4439.4333	1.9261	5.4276	25.5727	9.2411	13.4288
S4	98.3761	4337.6951	2.0534	6.4942	44.3990	8.8141	11.5275
S5	154.5770	11906.1778	2.6902	5.2868	38.3868	8.6098	8.9678
S6	92.1070	3928.2737	1.8817	5.0443	26.6131	9.4471	14.3211
S7	58.9136	1538.0087	1.5983	8.8093	45.4096	9.7930	19.8202
S8	113.5011	3729.0304	1.9431	7.3813	40.7545	9.1167	13.6220
S9	123.9228	4772.6962	1.9627	6.4519	26.4491	8.9417	13.3777
S10	104.4412	5035.6675	2.4088	5.5477	22.0450	8.7316	13.0023
S11	88.0243	4983.4344	2.1543	1.8514	5.5835	8.9289	13.6586
S12	56.3139	929.1097	1.4800	7.3944	49.8043	8.8109	13.3397

5. Conclusions

A constitutive model consisting of seven parameters for describing the stress–strain relationships of warp-knitted spacer fabrics was proposed. A parametric study was conducted to assess the effect of each parameter on the resultant stress–strain curve. Experimental validation was also carried out using twelve warp-knitted spacer fabrics. The analyses have showed that all the seven parameters have quantitatively effect on a particular phase of the resultant stress–strain curves of warp-knitted spacer fabrics. The change of each parameter makes a clear physical sense on the stress–strain curve. The proposed constitutive model yields much better fitting results than the existing constitutive models for polymeric or metallic foams. In particular, Parameter A is successfully defined as the plateau stress of warp-knitted spacer fabrics. The regressive stress–strain curves by the proposed constitutive model are very accurate and can be used for further theoretical analysis and application. This constitutive model will interest industrialists possessing a large number of experimental data to establish their empirical formulas to engineer the cushioning properties of warp-knitted spacer fabrics. In Part II, the constitutive model will be used to develop a dynamic model for predicting the impact compressive responses of warp-knitted spacer fabrics under various loading conditions.

References

1. Bagherzadeh R, Gorji M, Latifi M, et al. Evolution of moisture management behavior of high-wicking 3d warp knitted spacer fabrics. *Fiber Polym* 2012; 13: 529–534.

2. Dlugosch S, Hu H and Chan CK. Thermal comfort evaluation of equestrian body protectors using a sweating manikin. *Cloth Textiles Res J* 2013; 31: 231–243.

3. Liu YP, Hu H, Zhao L, et al. Compression behavior of warp-knitted spacer fabrics for cushioning applications. *Text Res J* 2012; 82: 11–20.

4. Liu YP, Hu H, Long HR, et al. Impact compressive behavior of warp-knitted spacer fabrics for protective applications. *Text Res J* 2012; 82: 773–788.

5. Liu YP and Hu H. An experimental study of compression behavior of warp-knitted spacer fabric. *J Eng Fiber Fabr* 2014; 9: 61–69.

6. Du ZQ and Hu H. A study of spherical compression properties of knitted spacer fabrics part I: theoretical analysis. *Text Res J* 2012; 82: 1569–1578.

7. Du ZQ and Hu H. A study of spherical compression properties of knitted spacer fabrics part II: comparison with experiments. *Text Res J* 2012; 83: 794–799.

8. Liu YP, Au WM and Hu H. Protective properties of warp-knitted spacer fabrics under impact in hemispherical form. Part I: impact behavior analysis of a typical spacer fabric. *Text Res J* 2014; 84: 422–434.

9. Liu YP, Hu H and Au WM. Protective properties of warp-knitted spacer fabrics under impact in hemispherical form. Part II: effects of structural parameters and lamination. *Text Res J* 2014; 84: 312–322.

10. Supeł B and Mikołajczyk Z. Model of the connector for 3D distance knitted fabric fastened by articulated joints. *Fibres Text East Eur* 2008; 16: 77–82.

11. Supeł B and Mikołajczyk Z. Model of the Compressing Process of a One- and Two-Side Fastened Connector of a 3D Distance Knitted Fabric. *Fibres Text East Eur* 2008; 16: 44–48.

12. Supeł B and Mikołajczyk Z. Modelling the process of the compression of distance knitted fabrics in the aspect of 'elastica curves'. *Fibres Text East Eur* 2010; 18: 52–55.

13. Mokhtari F, Shamshirsaz M, Latifi M, et al. Compressibility behaviour of warp knitted spacer fabrics based on elastic curved bar theory. *J Eng Fiber Fabr* 2011; 6: 23–33.

14. Vassiliadis S, Kallivretaki A, Psilla N, et al. Numerical modelling of the compressional behaviour of warp-knitted spacer fabrics. *J Eng Fiber Fabr* 2009; 17: 56–61.

15. Brisa VJD, Helbig F and Kroll L. Numerical characterisation of the mechanical behaviour of a vertical spacer yarn in thick warp knitted spacer fabrics. *J Ind Text*. Epub ahead of print. DOI: 10.1177/1528083714523164.

16. Hou X N, Hu H and Silberschmidt V. A study of computational mechanics of 3D spacer fabric: factors affecting its compression deformation. *J Mater Sci* 2012; 47: 3989–3999.

17. Liu QL and Subhash G. A phenomenological constitutive model for foams under large deformations. *Polym Eng Sci* 2004; 44: 463–473.

18. Avalle M, Belingardi G and Ibba A. Mechanical models of cellular solids: Parameters identification from experimental tests. *Int J Impact Eng* 2007; 34: 3–27.

19. Li C, Wang ZH, Zhao LM, et al. A Phenomenological Constitutive Model of Aluminum Alloy Foams at Various Strain Rates. *Int J Mod Phys B* 2008; 22: 6135–6140.